Infrared Matrix Isolation Study of the Thermal and Photochemical Reactions of Ozone with Dimethylzinc

Priya Varma and Bruce S. Ault*

Department of Chemistry, University of Cincinnati, P. O. Box 210172, Cincinnati, Ohio 45221-0172.

Received: January 22, 2008; Revised Manuscript Received: April 2, 2008

The matrix isolation technique has been combined with infrared spectroscopy and theoretical calculations to explore the reaction of $(CH_3)_2Zn$ with O_3 over a range of time scales. Upon twin jet deposition, an initial cage pair complex was observed, along with formation of the novel $H_3COZnCH_3$ species. Subsequent UV irradiation destroyed the complex and greatly increased the yield of $H_3COZnCH_3$. An extensive set of bands were seen for this molecule, and ^{18}O spectroscopic data were obtained as well. The identification of this species was supported by theoretical calculations at the B3LYP/6-311++g(d,2p) level. Merged jet deposition led to a very different set of products, including H_2CO, CH_3OH and C_2H_6, identifications that were confirmed by ^{18}O substitution. In addition, a new variable length concentric deposition technique was developed to permit study of the time scales between twin (relatively short) and merged (relatively longer) reaction times. Mechanistic inferences for this reaction are discussed.

Introduction

The application of semiconducting thin films in the microelectronics industry has completely revolutionized society, through the development of computers and a wide range of electronic devices. The importance of these films has led scientists and engineers to develop a variety of methods to produce these films.[1–3] These include electrolytic deposition from solution, plasma deposition, chemical vapor deposition (CVD), and atomic layer deposition (ALD).[4] ZnO is a wide band gap semiconductor that is routinely used as a transparent electrical contact, with many potential applications such as optical wave guides, UV lasers, and short-wavelength light emitting diodes (LEDs). ZnO is especially attractive for UV laser applications[4] due to its band gap of 3.37 eV and high exciton binding energy of 60 meV. One of the requirements for ALD or CVD fabrication of thin films is the availability of a volatile precursor of the metal, typically an organometallic compound. For example, dimethyl zinc, $(CH_3)_2Zn$ (Me_2Zn), is frequently employed for ZnO synthesis, along with O atoms from O_2 or H_2O as the oxygen source. In addition, Driess and co-workers[5,6] have experimentally studied the Me−Zn−O system in recent years as a means of synthesizing ZnO nanoparticles. In the past 5 years, the search for a better oxygen source has led researchers to ozone, O_3. However, relatively little is known about the gas or condensed-phase reactions of Me_2Zn with O_3. Just one study has been reported to date, a flow reactor study of the emission from the gas-phase reaction, in an effort to produce an electronic transition chemical laser.[7] Emission between 370 and 450 nm was identified as the cool blue emission of H_2CO. Beyond this, no mechanistic data were obtained, and initial intermediates were not seen.

The matrix isolation technique[8–11] was developed to facilitate the isolation and spectroscopic characterization of reactive intermediates and has been applied to the study of diverse species, including radicals, ions, and weakly bound molecular complexes. This approach, combined with theoretical calculations, may provide access to the study of initial intermediates in the above reactions and shed light on the mechanism of reaction of Me_2Zn with O_3 and O atoms. The present manuscript reports a study of merged jet (thermal) and twin jet (photochemical) reactions of Me_2Zn and O_3 with trapping in cryogenic matrices, as well as a new modified deposition approach, a variable distance concentric deposition device.

Experimental Section

All of the experiments in this study were carried out on a conventional matrix isolation apparatus that has been described.[12] Dimethyl zinc (Strem Chemical) was introduced into the vacuum system from lecture bottles into the vacuum system and was purified by freeze−pump−thaw cycles at 77 K. O_3 was produced by Tesla coil discharge of O_2 (Wright Brothers) and trapping at 77 K to remove residual O_2 and trace gases. $^{18}O_3$ was produced in the same manner from ^{18}O-labeled O_2 (94%, Cambridge Isotope Laboratories). Argon (Wright Brothers) was used as the matrix gas without further purification.

Matrix samples were deposited in three different modes: twin jet, merged jet, and a new concentric jet mode. In the first, the two gas samples were deposited from separate nozzles onto the 14 K window, allowing for only a brief mixing time prior to matrix deposition. Several of these matrices were subsequently warmed to 33−35 K to permit limited diffusion and then recooled to 14 K and additional spectra recorded. In addition, many of these matrices were irradiated for 1.0 h or more hours with either the H_2O/Pyrex-filtered or the H_2O/quartz-filtered output of a 200 W medium-pressure Hg arc lamp, after which additional spectra were recorded.

A number of experiments were conducted in the merged jet mode,[13] in which the two deposition lines were joined with an UltraTorr tee at a distance from the cryogenic surface, and the flowing gas samples were permitted to mix and react during passage through the merged region. To more effectively model the gas phase, the merged region was constructed of Teflon FEP, either $^1/_4$ or $^1/_8$ in. o.d. in a number of experiments. Copper tubing of $^1/_4$ in. o.d. was used in other additional experiments. The length of the merged region (or reaction zone) was varied from as short as 6 cm to as long as 70 cm.

* Corresponding author.

10.1021/jp800622j CCC: $40.75
Published on Web 05/31/2008

Twin jet and merged jet deposition probe different time scales for reaction, very short for twin jet and somewhat longer for merged jet. As will be reported below, quite different results were obtained with these two modes. To probe the intermediate time scale between twin and merged jet, a new concentric jet device was developed. In this approach, an $^1/_8$ in. o.d. Teflon FEP tube was inserted inside of a larger, $^1/_4$ in. o.d. tube, also Teflon FEP. The length of the $^1/_8$ in. tube could be adjusted to be shorter, longer, or the same as the outer tube. The distance between the outlet ends of the two tubes is referred to as $\Delta d =$ (position of inner tube) − (position of outer tube). $d > 0$ indicates that the inner tube extends beyond the outer tube, and $d < 0$ indicates that the inner tube is shorter than the outer tube (more like merged jet). $d = 0$ indicates that the ends of the two tubes are at the same distance from the cold window. Mixing of the two samples begins at the outlet of the inner tube and continues until deposition onto the cold window (typically 2−3 cm). In this manner, the time scale available for reaction could be adjusted from nearly that of the merged jet to nearly that of the twin jet. In all three deposition modes, matrices were deposited at the rate of 2 mmol/h from each sample manifold onto the cold window. Final spectra were recorded on a Perkin-Elmer Spectrum 2000 Fourier transform infrared spectrometer at 1 cm^{-1} resolution.

Theoretical calculations were carried out on likely intermediates in this study, using the Gaussian 03 and 03W suite of programs.[14] Density functional calculations using the hybrid B3LYP functional were used to locate energy minima, determine structures, and calculate vibrational spectra. Final calculations with full geometry optimization employed the 6-311 ++g(d, 2p) basis set, after initial calculations with smaller basis sets, were run to approximately locate energy minima. Thermodynamic functions for the reactants and potential intermediates were also calculated.

Results

Prior to any co-deposition experiments, blank experiments were run on each of the reagents used in this study. In addition, a blank of C_2H_6 in argon was run to provide an authentic spectrum for comparison to spectra recorded in this study. In each case, the blanks were in good agreement with literature spectra, and with blanks run previously in this laboratory.[15–17] Each blank experiment was then irradiated by the H_2O/Pyrex-filtered output of a 200 W Hg arc lamp for 1.0 h, and no changes were noted.

$(CH_3)_2Zn$ + O_3, Merged Jet. In an initial merged jet experiment, a 55 cm length of $^1/_4$ in. o.d. Teflon FEP tubing was used for the merged region or reaction zone. In this experiment, sample concentrations were $Ar/Me_2Zn = 250$ and $Ar/O_3 = 250$. Numerous product bands were seen in the final spectrum from this experiment, ranging from very intense bands (e.g., 1742 and 1499 cm^{-1}) to quite weak bands. All of the product bands seen in this experiment are listed in Table 1. The spectrum of this matrix sample is shown in Figure 1. In addition, parent bands of O_3 at 704 and 1043 cm^{-1} were observed, with intensities much less than those seen in blank experiments at the same concentration. Bands due to parent Me_2Zn were essentially absent in this experiment, indicating that extensive reaction had occurred.

Numerous additional merged jet experiments were conducted using the 55 cm long reaction zone. In these experiments, the absolute and relative concentrations of the two reagents were varied in a systematic manner. Relative concentrations ranged from 2:1 to 1:2, and absolute concentrations ranged from 500:1:1 to 2000:1:1. Throughout these experiments, the same set of product bands listed in Table 1 was observed. Moreover, the intensities of these bands varied directly with the total absolute concentrations employed; i.e., higher concentrations led to greater band intensities. In addition, the relative intensities of the product bands appeared to remain constant, to the degree that the weaker and overlapped bands could be measured accurately.

TABLE 1: Product Bands Positions, Intensities, and Assignments from the Merged-Jet Co-deposition of Ar/$(CH_3)_2Zn$ = 250 with Ar/O_3 = 250

band position, cm^{-1}			
^{16}O	^{18}O	intensity	assignment
821	821	m	C_2H_6
1033	1008	s	CH_3OH
1169	1168	m	H_2CO
1206	1186	w	
1245	1239	w	H_2CO
1335	1335	w	CH_3OH
1349	1349	w	CH_3CHO
1374	1374	w	C_2H_6
1466	1466	m	C_2H_6
1474	1474	w	CH_3OH
1499	1489	s	H_2CO
1728	1696	m	$[H_2CO]_2$ or CH_3CHO?
1742	1709	vs	H_2CO
1764	1735	mw	HCOOH?
2719	2708	w	CH_3CHO?
2746	2746	w	
2798	2798	vs	H_2CO
2864	2849	s	H_2CO
2893	2893	m	C_2H_6
2955	2955	m	C_2H_6
2962	2962	m	C_2H_6, CH_3OH
2980	2980	w	
3005	3005	w	CH_3OH
3464	3449	w	H_2CO ($2\nu_2$)
3667	3656	m	CH_3OH

Several experiments were conducted to explore the product yield as a function of the length and diameter of the reaction zone prior to deposition. In these experiments, the length was varied from 55 to 20 cm, and both $^1/_8$ and $^1/_8$ in. diameter Teflon FEP tubing were used. In these experiments, the bands listed in Table 1 were observed, and with approximately the same yield. Small variations in yield were seen in some experiments. However, these were not systematic with a change in reaction zone length and probably reflect slight variations in sample concentrations and flow rates (particularly O_3 samples, which can slowly lose O_3 to the walls of the sample during the course of an experiment). Also, a number of experiments were run using copper tubing for the reaction zone, instead of Teflon FEP. Again, the product bands, yield, and distribution were comparable to those described above at fixed concentrations, suggesting that the wall material is unimportant in these particular reactions and that the products are forming via gas-phase reactions.

A parallel set of experiments was conducted with samples of $Ar/^{18}O_3$ and $Ar/(CH_3)_2Zn$ in the merged jet mode with a 55 cm Teflon reaction zone. As anticipated, extensive reaction was observed so that very little of either parent species was observed in the resulting spectrum. Rather, an extensive set of product bands was observed. A number of these were shifted relative to the $^{16}O_3$ experiments described above, while several of the bands were unshifted. In addition, for the bands that shifted, weak bands were noted at the position of the ^{16}O product. For example, the 1742 cm^{-1} band reported above shifted to a strong band at 1709 cm^{-1} with $^{18}O_3$. A weak band was nonetheless

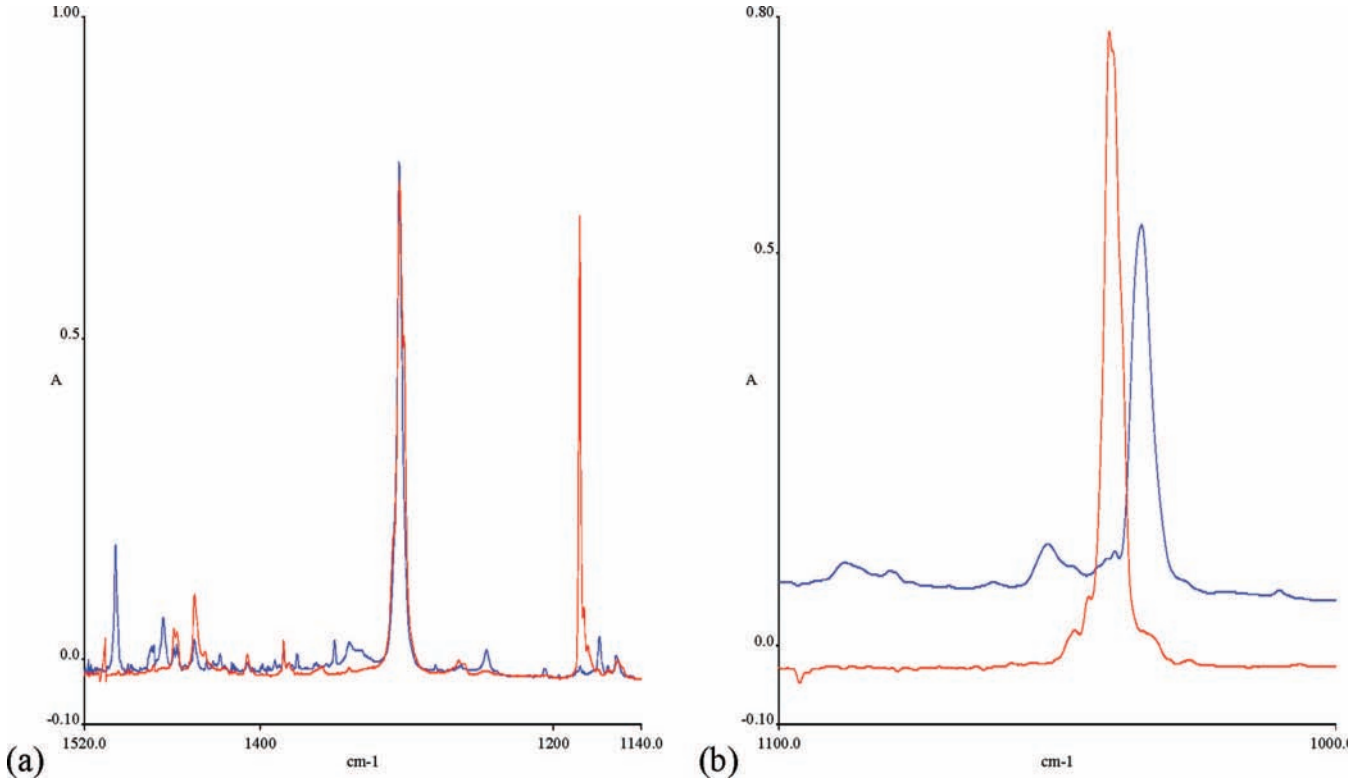

Figure 1. Infrared spectra after merged jet deposition of a sample of Ar/$(CH_3)_2Zn$ = 500 with a sample of Ar/O_3 = 250. Panel a shows the region of 1140−1520 cm^{-1} for this sample (blue) and a blank of $(CH_3)_2Zn$ (red), including the 1499 cm^{-1} band of H_2CO, and the loss of the parent Me_2Zn band at 1180 cm^{-1}. Panel b shows the region of 1000−1100 cm^{-1} for this sample (top, blue) and a blank of O_3 (bottom, red) showing the loss of the O_3 parent band and growth of the C−O stretch of CH_3OH.

observed at 1742 cm^{-1} due to residual ^{16}O in the $^{18}O_3$ sample. These results were reproduced in several subsequent experiments. Product band positions in the $^{18}O_3$ experiments are also listed in Table 1.

$(CH_3)_2Zn + O_3$, Twin Jet. In general, quite different results were obtained in the twin jet experiments compared to the results described above for merged jet. In an initial experiment, a sample of Ar/$(CH_3)_2Zn$ = 250 was co-deposited with a sample of Ar/O_3 = 250 using twin jet deposition. Several weak bands were observed upon initial deposition, *none of which coincide with product bands in the merged jet experiments*. The most intense of these was located at 1090 cm^{-1}, followed by a band at 2815 cm^{-1}. This matrix was then irradiated for 2 h with light of $\lambda > 200$ nm. A few of the bands present before irradiation decreased or were destroyed by irradiation. These will be referred to as set A. An additional set of the weak bands present before irradiation grew greatly as a result of irradiation, and will henceforth be called set B. Finally, a number of additional weak bands appeared upon irradiation. These may be associated with set B as well, but were too weak to be detected prior to irradiation. These bands did not coincide with any of the product bands in the merged jet experiments. The bands of sets A and B are listed in Table 2 and shown in Figure 2.

Twin jet experiments on this system were repeated numerous times, varying the concentration of the two reagents. The results described above were reproduced in all of these experiments. The same product bands were seen before and after irradiation, with intensities that were directly proportional to sample concentrations. In addition, the relative intensities of the initial product bands and those formed or increased upon irradiation remained constant from one experiment to the next, with the two groups (sets A and B).

A similar set of twin jet experiments was conducted with samples of Ar/$(CH_3)_2Zn$ and Ar/$^{18}O_3$ made from $^{18}O_2$ containing approximately 94% ^{18}O. Upon initial sample deposition, similar weak product bands were observed, in a number of cases shifted somewhat from the positions with ^{16}O. For example, the 1090 cm^{-1} band shifted to 1060 cm^{-1}, while the 2815 cm^{-1} band did not shift at all. In some cases, the weak product bands could not be observed due to overlap with the intense parent peaks. After irradiation, the set A bands again decreased, while the set B bands grew substantially. All of these are listed in Table 2. Of particular importance, sufficient ^{16}O remained in this $^{18}O_3$

TABLE 2: Product Band Positions[a] in the Twin-Jet Deposition of Ar/$(CH_3)_2Zn$ with Ar/O_3 before and after Irradiation

band position, cm^{-1}			
^{16}O	^{18}O	irradiation behavior	assignment
526	515	↑	$H_3COZnCH_3$
638		↓	complex/cage pair
869		↓	complex/cage pair
975	949	↓	complex/cage pair
1078[b]		↑	$H_3COZnCH_3$ (second site)
1090	1060	↑	$H_3COZnCH_3$
1175	1168	↓	complex/cage pair
1195	1189	↑	$H_3COZnCH_3$
1273[b]	1270	↑	$H_3COZnCH_3$ (second site)
1280	1277	↑	
1346[b]		↑	
1452[b]	1451	↑	$H_3COZnCH_3$
2815	2815	↑	$H_3COZnCH_3$
2877[b]	2877	↑	$H_3COZnCH_3$
2883[b]	2882	↑	$H_3COZnCH_3$ (second site)
2896	2895	↑	$H_3COZnCH_3$
2932	2931	↑	$H_3COZnCH_3$
2942[b]	2941	↑	$H_3COZnCH_3$ (second site)
2948	2948	↑	$H_3COZnCH_3$

[a] Band positions in cm^{-1}. [b] Not observed before irradiation.

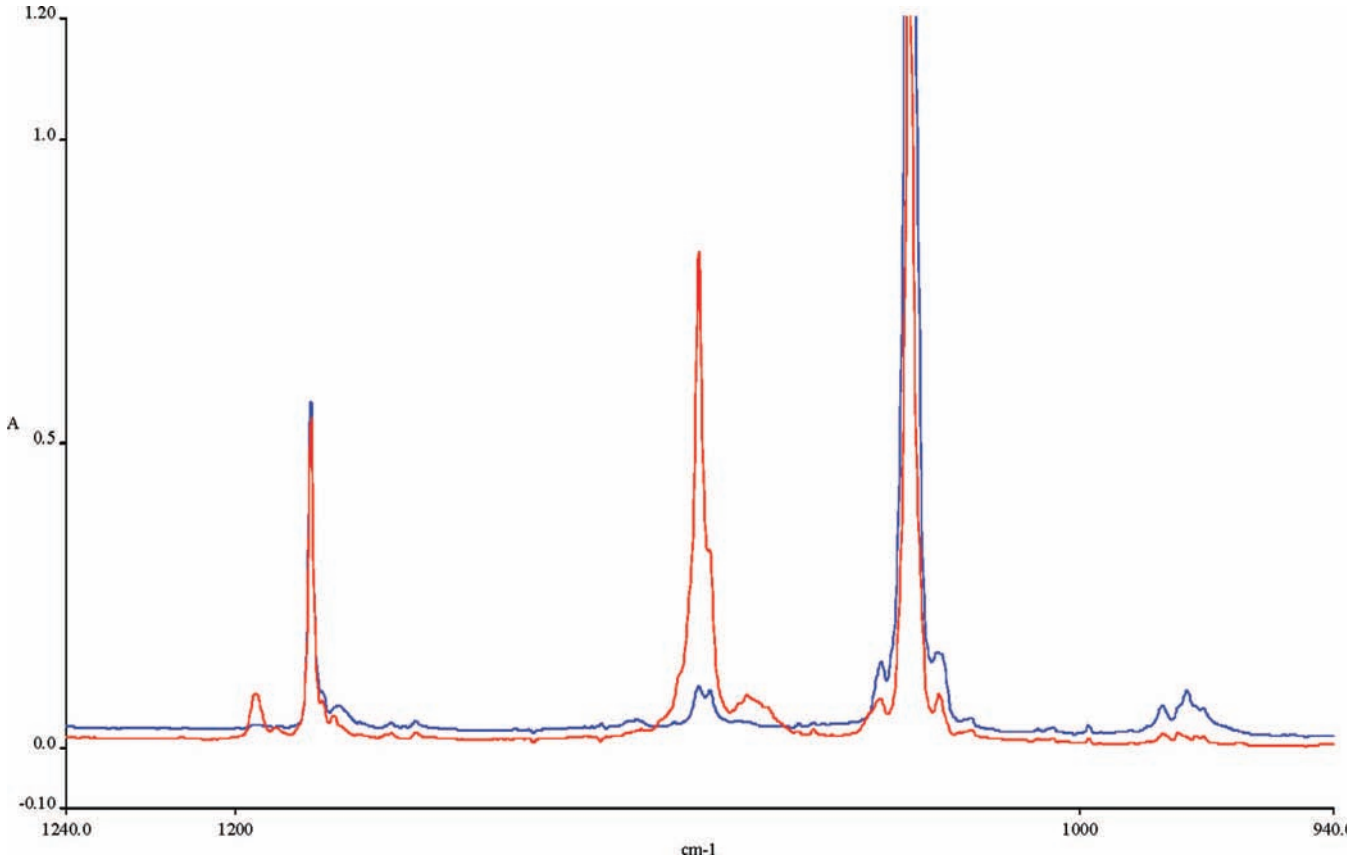

Figure 2. Infrared spectra from 940 to 1140 cm^{-1} after twin jet deposition of a sample of $Ar/(CH_3)_2Zn$ and Ar/O_3, before and after irradiation. Note the growth of the bands at 1090 and 1195 cm^{-1} and decrease of the band at 975 cm^{-1}.

sample such that a small amount of the ^{16}O product was weakly observed for several products. These include the $^{16}O/^{18}O$ pairs at 526/514, 1090/1060, and 1193/1189 cm^{-1}. No intermediate bands were observed between the position of the ^{16}O product and the ^{18}O product. These results were reproduced in each experiment, with a variation in product band intensities that was proportional to the reagent concentrations.

$(CH_3)_2Zn + O_3$, Concentric Jet. The reaction of these two species was explored in several concentric jet experiments as well, all with concentrations of 250:1 for each reagent, and d ranging from −5.0 to +1.3 cm. In an experiment with $d = +1.3$ cm, the bands seen in the twin jet experiments (sets A and B) were seen very clearly with yields similar to those in the twin jet experiments. However, the most intense band seen in the merged jet experiments, at 1742 cm^{-1}, was seen only very weakly in this experiment, and none of the remainder of the bands in the merged jet experiments were observed. When an experiment was conducted with $d = 0$, similar results were obtained, with a slightly increased yield of the sets A and B bands, and very low intensity for the 1742 cm^{-1} merged jet band. In contrast, in an experiment with $d = -1.3$ cm, sets A and B bands had similar intensity, while the 1742 cm^{-1} band grew substantially along with the more intense of the bands seen in the merged jet experiments. Additional experiments were conducted with $d = -2.5$ and −5.0 cm. In these experiments, set A and B bands were about the same intensity, while the bands due to the merged jet products grew greatly. The experiment with $d = -5.0$ cm resembled closely the merged jet experiments described above. No new bands (i.e., bands not seen in either the twin or merged jet experiments) were seen in any of these experiments. Table 3 compares product band intensities as a function of d, while Figure 3 shows spectra with $d = +1.3$ and −1.3 cm.

TABLE 3: Product Ratios[a] in Concentric Jet Experiments as a Function of *d*

d, cm	*I*(1090 cm^{-1}), O.D.	*I*(1742 cm^{-1}), O.D.	ratio *I*(1090)/*I*(1742)
+1.3	0.048	0.013	3.69
0.0	0.079	0.012	6.58
−1.3	0.044	0.113	0.39
−2.5	0.042	0.159	0.26
−5.0	0.039	0.329	0.12
−55[b]	0.002	0.81	0.003

[a] 1090 cm^{-1} absorption of $H_3COZnCH_3$ compared to 1742 cm^{-1} absorption of H_2CO. [b] From merged jet experiment with 55 cm reaction zone.

Results of Calculations

Likely radical and closed shell products arising from the reaction of $(CH_3)_2Zn$ with O_3 were considered. Many possible products are known species for which experimental spectra are available for comparison. For possible products that are not well-known and characterized spectroscopically, theoretical calculations using density functional methods were carried out to locate potential energy minima and compute infrared spectra, including ^{18}O isotopic shifts. These included CH_3Zn, $H_3COZnCH_3$, and similar molecules. All of the species under consideration optimized to energy minima on their respective potential energy surfaces, with all positive vibrational frequencies. Of particular interest was $H_3COZnCH_3$, for which there has been one previous theoretical report concerning the monomer and the tetramer,[18] and for which the tetramer has been synthesized,[19] but not the monomer. The structure calculated here at the B3LYP/6-311++g(d,2p) level agreed very well with the calculated structure in this previous report, particularly the slightly bent geometry at the Zn center (here 174.7° versus 174.3° in the

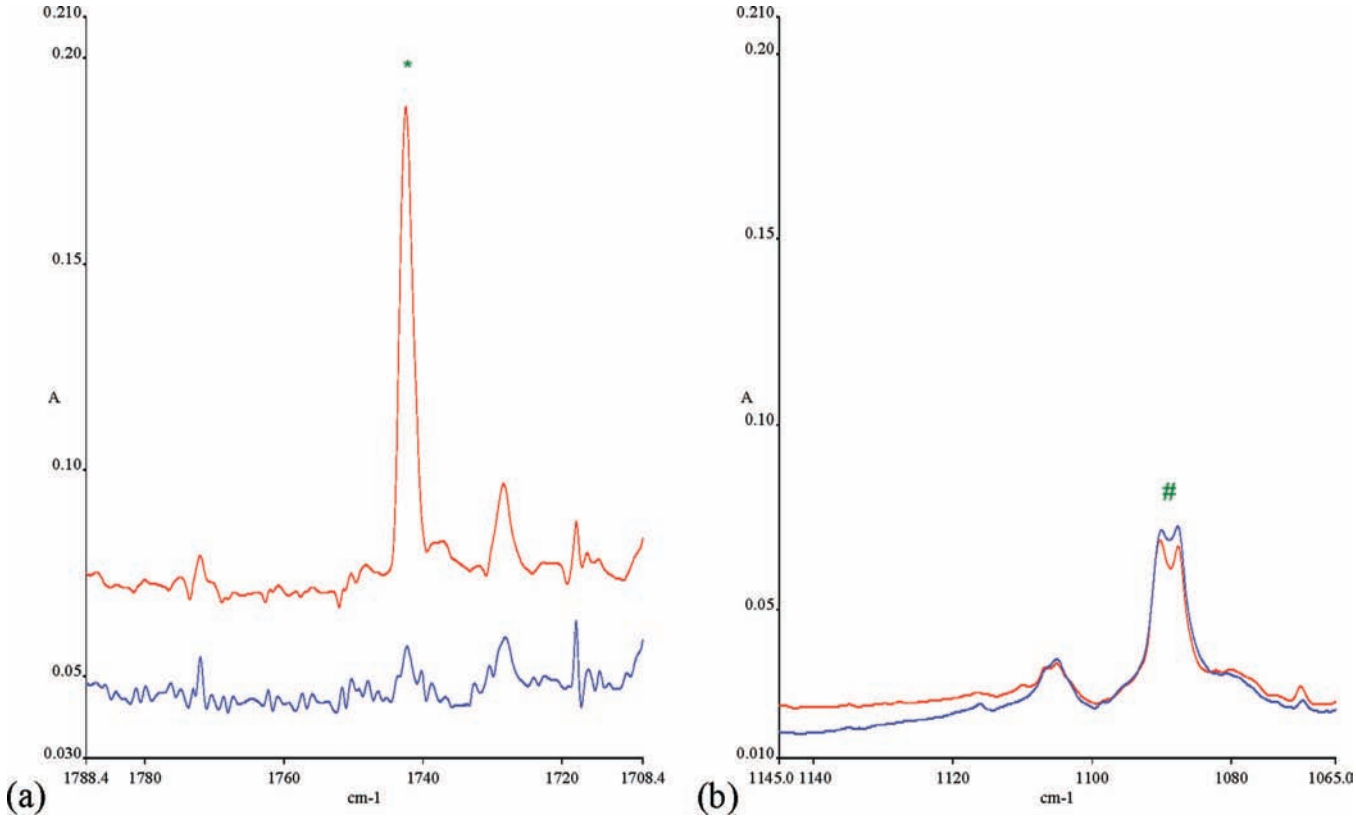

Figure 3. Comparison of spectra between 1708−1788 and 1065−1145 cm^{-1} after concentric jet deposition, as a function of *d*. In the blue (lower) trace $d = +1.3$ cm, and in the upper (red) trace, $d = -1.3$ cm. The 1742 cm^{-1} band of H_2CO is noted with ∗ in a, and the 1090 cm^{-1} band of $H_3COZnCH_3$ is noted with a # in b.

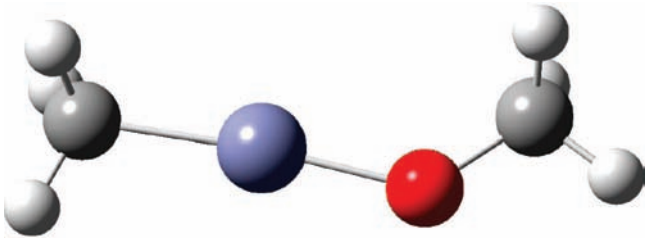

Figure 4. Structure of $H_3COZnCH_3$, computed at the B3LYP/6-311++g(d,2p) level of theory. Note the slightly nonlinear (174.7°) C−Zn−O angle. Additional structural parameters of interest: *R*(C−Zn) = 1.935 Å, *R*(Zn−O) = 1.789 Å, *R*(O−C) = 1.411 Å, *R*(C−H) = 1.09 Å, and α(Zn−O−C) = 131.3°.

previous report at the B3LYP/6-311++g(3df,3pd) level). The spectrum calculated here agreed within a few cm^{-1} of the previous report; the calculated spectrum of the ^{18}O species was also carried out here. The calculated structure is represented in Figure 4, and the calculated spectrum is listed in Table 4.

TABLE 4: Comparison of Experimental and Calculated Bands and Isotopic Shifts for $H_3COZnCH_3$

CH_3OZnCH_3						
calcd freq[a,b]	*I*[c]	exptl freq	^{18}O calcd		calcd shift	exptl shift
494.4	10	526	483.6	12	−9	−11
629.2	49		619.8	46	−9	
724.2	35		723.9	34	0	
726.2	32		726.0	32	0	
1109.2	273	1090	1076.5	258	−33	−30
1165.7	0		1163.0	0	−3	
1186.2	20	1195	1180.9	7	−5	−6
1220.5	2		1220.2	1	0	
1464.5	1		1464.5	1	0	
1465.9	1		1465.9	1	0	
1480.8	25	1452	1479.7	29	−1	−1
1500.7	2		1500.6	2	0	
1502.1	2		1502.0	2	0	
2957.2	142	2815	2957.2	142	0	0
2994.0	74		2994.0	74	0	
3028.8	60	2895	3028.7	60	0	−1
3032.5	13		3032.5	13	0	0
3107.7	9	2932	3107.7	9	0	−1
3109.6	9	2948	3109.6	9	0	0

[a] Band positions in cm^{-1}. [b] Calculated frequencies at the B3LYP/6-311++g(d,2p) level, unscaled. [c] Intensities in km/mol.

Discussion

Merged jet and twin jet deposition probe somewhat different time and temperature regimes with respect to the mixing and reacting of $(CH_3)_2Zn$ and O_3. Twin jet deposition allows for only a very brief mixing time on the surface of the condensing matrix surface, at temperatures below room temperature but above the 14 K temperature of the rigid matrix. Merged jet deposition allows for room temperature mixing and flow through the reaction zone before condensation into the matrix. The time available for reaction, on the order of milliseconds, is much longer than in the twin jet. For $(CH_3)_2Zn$ and O_3, quite different products were seen upon merged jet as compared to twin jet deposition. Concentric jet deposition was designed to probe the time regime intermediate between twin and merged jet deposition.

An extensive set of product bands was seen with merged jet deposition, as listed in Table 1. These product bands were nearly independent of the length of the merged region over the range of 20−55 cm and were likewise independent of the sample concentrations that were employed. A number of the product bands showed distinct shifts with ^{18}O substitution, indicating

the presence of one or more O atoms in the absorbing species, while other bands did not shift with ^{18}O substitution. For the more intense product bands in the ^{18}O experiments that did shift, a weak residual band at the ^{16}O band location was observed, with no intermediate bands (i.e., a 1709, 1742 cm^{-1} $^{18}O/^{16}O$ pair was seen, with no product bands between them). This indicates that there must be exactly one O atom in the absorbing species. Using these results and the observation made by Lee and Zare[7] that H_2CO emission was observed from gas-phase flames of Me_2Zn and O_3, product identifications can be made. In these merged jet experiments, all of the product bands can be assigned to known, stable species. All six fundamentals of H_2CO were seen,[20] dominated by the C═O stretch at 1742 cm^{-1} and followed by the CH_2 bend at 1499 cm^{-1}. In addition, several modes, including the C−O and O−H stretches, of CH_3OH were clearly observed,[21] along with their ^{18}O counterparts. Finally, one set of product bands did not shift with ^{18}O substitution. These match the most intense bands of ethane, C_2H_6 and are so assigned.[22] Beyond these three major products, a few weak bands remain. A few are close to bands of formic acid, HCOOH, and acetaldehyde, but their low intensity precludes definitive identification.[23,24] A potential product (see below) is $HZnCH_3$. However, the most intense band of this species has been identified[25] at 1867 cm^{-1} and is not observed here. As discussed below, the proposed mechanism involves radical formation and destruction, so the formation of radicals such as CH_3O, CH_2OH, CH_3, and CH_3Zn must be considered as well. The infrared spectra of the first three are known.[26−28] The weak bands observed here are near but not identical to bands of CH_3O and CH_2OH, so no firm conclusion may be reached as to whether these species are or are not present at low levels. The most intense absorption of CH_3 at 617 cm^{-1} overlaps nearly exactly a parent mode of $(CH_3)_2Zn$, so that it is difficult to draw any conclusions about this radical. However, in one experiment with O_3 in excess, the parent bands of Me_2Zn were nearly completely absent. In this experiment, a very weak absorption was then noted at 615 cm^{-1}. This could be due to a very small residual of Me_2Zn or a trace of CH_3. No definitive conclusion can be drawn. CH_3Zn has been observed by LIF in the gas phase,[30] providing some information about a few of the ground-state fundamentals of this species. This information is consistent with the spectrum calculated here for CH_3Zn. The calculations predict weak bands only and do not match well to the weak bands observed here. Hence, this species is likely not present.

The results in the twin jet experiments were quite different. First, only quite weak bands were observed upon initial deposition, consistent with the very brief mixing time and low mixing temperature. Second, none of the bands in the twin jet experiments matched bands observed in the merged jet experiments, indicating that the reaction was being quenched at an earlier step in the reaction sequence. The initial twin jet product bands could be sorted into two sets, A and B, on the basis of their behavior upon subsequent irradiation. The set A bands were diminished and in some experiments destroyed by UV irradiation, while the set B bands grew up to a factor of 10-fold as shown in Figure 2. The set A bands were generally near parent bands of either $(CH_3)_2Zn$ or O_3. Those set A bands near parent bands of Me_2Zn did not shift upon ^{18}O substitution, while those near parent bands of O_3 shifted strongly. These observations, combined with the photosensitivity of the set A bands, suggest that they are due to an initial weak complex formed between the two reactants, either by distinct chemical interaction or cage pairing in the argon matrix. The set B bands were present weakly initially and increased significantly upon irradiation and destruction of the initial complex. Additional weaker bands also grew in and are likely due to the species responsible for the set B bands. O_3 is known to be a good photochemical O atom source, suggesting that this absorber may be the product of the reaction of an O atom with Me_2Zn. Lee and Zare[7] proposed that the initial step in the gas phase reaction was insertion of an O atom into a Zn−C bond, forming excited CH_3O, presumably along with $ZnCH_3$. In the gas phase, this species could go on and react further, ultimately leading to the H_2CO emission observed by these researchers. However, in an argon matrix, excess energy is rapidly quenched by the matrix, and initially formed species cannot separate and diffuse apart. Radical recombination will then occur, and a likely product is $H_3COZnCH_3$. While this species has never been observed, its tetramer has been identified in previous studies.[19]

To complement the experimental data, density functional theory (DFT) calculations were carried out for $H_3COZnCH_3$, to determine the optimized structure and calculate the infrared spectrum of this species. An energy minimum was located, and the vibrational spectra of both the normal isotopic species and the ^{18}O-substituted species were calculated. As shown in Table 3, the agreement between experiment and calculation is excellent. The most intense band is calculated to come at 1109 cm^{-1} with a 33 cm^{-1} ^{18}O shift. The most intense band in the experimental spectrum came at 1090 cm^{-1}, with a 30 cm^{-1} isotopic shift. The second most intense band, the lowest frequency C−H stretch, was computed at 2957 cm^{-1} (harmonic frequency). With scaling due to anharmonicity, this matches well the second most intense experimental band, a C−H stretch at 2815 cm^{-1}. Overall, the agreement between the calculated spectrum, including isotopic shifts and relative intensities, and the experimental results is excellent. Consequently, the set B bands, including many of the weaker bands seen only after irradiation, are assigned to the oxidizing product $H_3COZnCH_3$.

Results from the concentric jet experiments support both the twin and merged jet results and provide insights into the intermediate time regime. With $d \geq 0$, the results were very similar to twin jet deposition with observation of bands due to $H_3COZnCH_3$ and the cage pair complex, with very little CH_2O. As d became negative, from −1.25 to −5.0 cm, the yield of CH_2O increased dramatically while the yield of $H_3COZnCH_3$ remained constant or declined slightly, very similar to merged jet deposition. Significantly, no new bands (other than those seen in twin and merged jet deposition experiments) were observed at any value of d, suggesting that *this technique is able to tune continuously from twin jet to merged jet deposition.* While no new intermediates were seen for this particular pair of reactants, concentric jet deposition may be quite valuable for a number of chemical systems.

Reaction Mechanism. The "snapshots" of the reaction at different times probed by twin jet, concentric jet, and merged jet deposition provide some insight into the mechanism of the reaction. As proposed by Lee and Zare, the first step appears to be oxidation of the Zn−C bond, forming H_3CO and (presumably) $ZnCH_3$ or Zn + CH_3

$$(CH_3)_2Zn + O_3 \rightarrow H_3CO^* + ZnCH_3 + O_2 \qquad (1a)$$

or

$$(CH_3)_2Zn + O_3 \rightarrow H_3CO + Zn + CH_3 + O_2 \qquad (1b)$$

Both of these steps are calculated to have $\Delta E_0^\circ < 0$, although only slightly so in the case of reaction 1b. In the matrix or in the relatively dense region immediately in front of the condensing matrix, these recombine to form the observed $H_3COZnCH_3$

product, while in the gas phase they separate and react further. It is interesting that a small amount of $H_3COZnCH_3$ is formed upon initial deposition, before irradiation. This must occur late in the matrix condensation process, just as the matrix is becoming rigid, so that the two radicals cannot diffuse apart and be trapped in separate cage sites.

The major products formed in the merged jet experiments are all stable, known species which must be accounted for in the reaction mechanism. Lee and Zare suggested that the following reaction occurs to account for the electronically excited H_2CO they observed:

$$H_3CO + H_3CO \rightarrow CH_3OH + H_2CO^* \quad (2)$$

Presumably other H atom acceptors (e.g., CH_3, $ZnCH_3$) could also react with H_3CO, leading to H_2CO formation. Step 2 accounts for the formation of two of the major observed products, methanol and formaldehyde. Since reaction 2 is second order in CH_3O, it requires a sufficient quantity of the methoxy radical to proceed. This, in turn, suggests that reaction 1 is very rapid at room temperature, in agreement with the results from this study and that of Lee and Zare.

Several questions remain about the mechanism: How is C_2H_6 formed in this reaction? What is the fate of Zn in the gas-phase reaction? How do the minor products form? Although CH_3 radicals were not detected, possibly due to band overlap with Me_2Zn, the following may occur:

$$CH_3 + CH_3 + Ar \rightarrow C_2H_6 + Ar \quad \Delta E_0^\circ = -82.0 \text{ kcal/mol} \quad (3a)$$

$$CH_3 + CH_3Zn \rightarrow C_2H_6 + Zn \quad \Delta E_0^\circ = -71.3 \text{ kcal/mol} \quad (3b)$$

$$CH_3 + CH_3Zn \rightarrow H_2C{=}Zn + CH_4 \quad \Delta E_0^\circ = -3.7 \text{ kcal/mol} \quad (3c)$$

$$CH_3Zn + CH_3Zn \rightarrow C_2H_6 + 2Zn \quad \Delta E_0^\circ = -60.7 \text{ kcal/mol} \quad (3d)$$

$$CH_3Zn + CH_3Zn \rightarrow H_3C{-}Zn{-}Zn{-}CH_3 \quad \Delta E_0^\circ = -52.4 \text{ kcal/mol} \quad (3e)$$

(all ΔE_0° values calculated at the B3LYP/6-311++g(d,2p) level of theory). Reactions 3a, 3b, and 3d provide viable pathways for the formation of C_2H_6 and cannot be distinguished with the available data, while reaction 3c provides an alternative route for the disappearance of CH_3, and reaction 3e provides an alternative route for the disappearance of CH_3Zn. However, these reactions are energetically less favorable than their counterpart reactions 3b and 3d. More importantly, the calculated spectra of $H_2C{=}Zn$ and $H_3C{-}Zn{-}Zn{-}CH_3$ were not consistent with the observed spectra, while C_2H_6 was experimentally observed.

While Zn is clearly present in the twin jet experiments as $H_3COZnCH_3$, its fate is not as apparent in the merged jet experiments. No Zn-containing products were observed in these experiments. Many of these would be very weak infrared absorbers and might have escaped detection. Of course, Zn and Zn_2 are infrared-inactive. If formed through reactions 1b, 3b, or 3d, they would not be observed spectroscopically. It is noteworthy that Lee and Zare[7] observed Zn atom emission, as well as ZnH emission, from the reaction of O_3 with $(C_2H_5)_2Zn$. Finally, ZnO and $HZnCH_3$ are also reasonable products in this system. Little is known about the spectrum of ZnO. It has been reported at 811 cm^{-1} in N_2 matrices,[29] with a 40 cm^{-1} ^{18}O shift. The argon matrix positions are likely to shift slightly, but should be in the same region. No absorptions were observed which could be attributed to ZnO. As noted above, $HZnCH_3$ was not observed in the present study. The most likely explanation for the fate of zinc under the present reaction conditions is the formation of Zn atoms or dimers which are not observable spectroscopically.

Several weak bands due to minor products were seen in the merged jet experiments as well. These cannot be definitively identified due to the weakness of the absorptions, and probably arise from secondary reactions (i.e., reactions with additional molecules of either O_3 or Me_2Zn). Without more information, no mechanistic conclusions may be drawn about the formation of these minor products.

Conclusions

Merged jet co-deposition of reacting mixtures of Me_2Zn and O_3 in argon leads to the isolation of H_2CO, CH_3OH, and C_2H_6 as primary products, nearly independent of the length of the merged region. Twin jet deposition leads to initial formation of a cage pair complex (species A) along with a small amount of the oxidation product $H_3COZnCH_3$ (species B). The complex is destroyed by subsequent irradiation, while the yield of $H_3COZnCH_3$ is greatly enhanced. Concentric deposition provides a continuous transition from twin-jet-like to merged-jet-like conditions, allowing for simultaneous observation of both types of products. The data obtained here support a mechanism in which the initial step is the formation of an excited H_3CO radical from which H_2CO is formed via hydrogen atom loss and from which CH_3OH is formed through H atom addition.

Acknowledgment. The University of Cincinnati is gratefully acknowledged for their support of this research through a URC Grant to B.S.A. and a WISE (Women in Science and Engineering) fellowship to P.V. Initial guidance from Michael Hoops is also acknowledged.

References and Notes

(1) Scarel, G.; Debernardi, A.; Tsoutsou, D.; Spiga, S.; Capelli, S. C.; Lamagna, L.; Volkos, S. N.; Alia, M.; Fanciulli, M. *Appl. Phys. Lett.* **2007**, *91*, 102901/1.

(2) Dezelah, C. L., IV; Wiedmann, M. K.; Mizohata, K.; Baird, R. J.; Niinistoe, L.; Winter, C. H. *J. Am. Chem. Soc.* **2007**, *129*, 12370.

(3) Kwoka, M.; Ottaviano, L.; Szuber, J. *Thin Solid Films* **2007**, *515*, 8328.

(4) Barnes, T. M.; Leaf, J.; Hand, S.; Fry, C.; Wolden, C. A. *J. Appl. Phys.* **2004**, *96*, 7036–7044.

(5) Hambrock, J.; Rabe, S.; Merz, K.; Berkner, A.; Wolfart, A.; Fischer, R. A.; Driess, M. *J. Mater. Chem.* **2003**, *13*, 1731.

(6) Schroder, D.; Schwarz, H.; Polarz, S.; Driess, M. *Phys. Chem. Chem. Phys.* **2005**, *7*, 1049.

(7) Lee, H. U.; Zare, R. N. *Combust. Flame* **1975**, *24*, 27.

(8) Whittle, E.; Dows, D. A.; Pimentel, G. C. *J. Chem. Phys.* **1954**, *22*, 1943.

(9) Craddock, S.; Hinchliffe, A. *Matrix Isolation*; Cambridge University Press: Cambridge, U.K., 1975.

(10) *Chemistry and Physics of Matrix Isolated Species*; Andrews, L., Moskovitz, M. Eds.; Elsevier Science: Amsterdam, 1989.

(11) Dunkin, I. R. *Matrix Isolation Techniques, a Practical Approach*; Oxford University Press: New York, 1998.

(12) Ault, B. S. *J. Am. Chem. Soc.* **1978**, *100*, 2426.

(13) Carpenter, J. D.; Ault, B. S. *J. Phys. Chem.* **1991**, *95*, 3502.

(14) Frisch, M. J.; Trucks, G. W.; Schlegel, H. B.; Robb, M. A.; Cheeseman, J. R.; Montgomery, J. A., Jr.; Vreven, T.; Kudin, K. N.; Burant, J. C.; Millam, J. M.; Iyengar, S. S.; Tomasi, J.; Barone, V.; Mennucci, B.; Cossi, M.; Scalmani, G.; Rega, N.; Petersson, G. A.; Nakatsuji, H.; Hada, M.; Ehara, M.; Toyota, K.; Fukuda, R.; Hasegawa, J.; Ishida, M.; Nakajima, T.; Honda, Y.; Kitao, O.; Nakai, H.; Klene, M.; Li, X.; Knoz, J. E.; Hratchian, H. P.; Cross, J. B.; Adamo, C.; Jaramillo, J.; Gomperts, R.;

Stratmann, R. E.; Yazyev, O.; Austin, A. J.; Cammi, R.; Pomelli, C.; Ochterski, J. W.; Ayala, P. Y.; Morokuma, K.; Voth, G. A.; Salvador, P.; Dannenberg, J. J.; Zakrzewski, V. G.; Dapprich, S.; Daniels, A. D.; Strain, M. C.; Farkas, O.; Malick, D. K.; Rabuck, A. D.; Raghavachari, K.; Foresman, J. B.; Ortiz, J. V.; Cui, Q.; Baboul, A. G.; Clifford, S.; Cioslowski, J.; Stefanov, B. B.; Liu, G.; Liashenko, A.; Piskorz, P.; Komaromi, I.; Martin, R. L.; Fox, D. J.; Keith, T.; Al-Laham, M. A.; Peng, C. Y.; Nanayakkara, A.; Challacombe, M.; Gill, P. M. W.; Johnson, B.; Chen, W.; Wong, M. W.; Gonzalez, C. and Pople, J. A. *Gaussian 03*, Revision B.04; Gaussian: Pittsburgh, PA, 2003.

(15) Andrews, L.; Spiker, R.C. *J. Phys. Chem.* **1978**, *76*, 1978.

(16) Bochmann, M.; et al. *Spectrochim. Acta* **1992**, *48A*, 1173.

(17) Schriver, A. *Chem. Phys.* **2007**, *334*, 128.

(18) Steudel, R.; Steudel, Y. *J. Phys. Chem. A* **2006**, *110*, 8912.

(19) Coates, G. E.; Ridley, D. *J. Chem. Soc.* **1965**, 1860.

(20) Diem, M.; Lee, E. K. C. *J. Phys. Chem.* **1982**, *86*, 1982.

(21) Barnes, A. J.; Hallam, H. E. *Trans. Faraday Soc.* **1970**, *66*, 1920.

(22) Schriver, A.; Schriver-Mazzuoli, L.; Ehrenfruend, P.; d'Hendecourt, L. *Chem. Phys.* **2007**, *334*, 128.

(23) Gantenberg, M.; Halupka, M.; Sander, W. *Chem. Eur. J.* **2000**, *6*, 1865.

(24) Della Vedova, C. O.; Sala, O. *J. Raman Spectrosc.* **1991**, *22*, 505.

(25) Greene, T. M.; Andrews, L.; Downs, A. J. *J. Am. Chem. Soc.* **1995**, *117*, 8180.

(26) Ciang, S.-Y.; Hsu, Y.-C.; Lee, Y.-P. *J. Chem. Phys.* **1989**, *90*, 81.

(27) Jacox, M. E. *Chem. Phys.* **1981**, *59*, 213.

(28) Jacox, M. E. *J. Mol. Spectrosc.* **1977**, *66*, 272.

(29) Povey, I. M.; Bezant, A. J.; Corlett, G. K.; Ellis, A. M. *J. Phys. Chem.* **1994**, *98*, 10427.

(30) Prochaska, E.; Andrews, L. *J. Chem. Phys.* **1980**, *72*, 6782.

JP800622J